Structural changes in bunched crystalline ion beams

2003 J. Phys. A: Math. Gen. 36 6119

(http://iopscience.iop.org/0305-4470/36/22/339)

INSTITUTE OF PHYSICS PUBLISHING JOURNAL OF PHYSICS A: MATHEMATICAL AND GENERAL

J. Phys. A: Math. Gen. **36** (2003) 6119–6127 PII: S0305-4470(03)55116-2

Structural changes in bunched crystalline ion beams

M Bussmann, U Schramm, T Schätz[1] and D Habs

Sektion Physik, Ludwig Maximilians Universität München, Germany

E-mail: ulrich.schramm@physik.uni-muenchen.de

Received 22 October 2002, in final form 9 December 2002
Published 22 May 2003
Online at stacks.iop.org/JPhysA/36/6119

Abstract

Measurements of the spatial distribution of bunched crystalline ion beams in the radio frequency quadrupole storage ring PALLAS are presented for different ratios of the longitudinal and the transverse confinement strengths.

The length of highly elongated crystalline ion bunches and its dependence on the bunching voltage is compared to predictions for a one-dimensional ion string and three-dimensional space-charge-dominated beams. The length is found to be considerably shorter than that predicted by the models. Furthermore, the scaling of the length with the bunching voltage is shown to differ from the expected inverse cube root scaling. These differences can partially be attributed to the formation of a mixed crystalline structure.

Additionally, a concise mapping of the structural transition from a string to a zig-zag configuration as a function of the ratio of the confinement strengths is presented, which in a similar way deviates from the predictions.

PACS numbers: 29.20.Dh, 41.75.−I, 52.27.Gr, 05.70.Fh

1. Introduction

In the PALLAS (PAuL Laser cooling Acceleration System) rf quadrupole storage ring [1], crystalline ion beams [2–4] have recently been experimentally realized at a beam energy of around 1 eV [1, 5–7]. Generally, the phase transition to the Coulomb-ordered 'crystalline' state, the state of ultimate brilliance, can occur when the mutual Coulomb energy of stored ions overcomes their mean kinetic energy by about two orders of magnitude. As typical inter-ion distances amount to the order of 10 μm, beam temperatures in the mK range are required to fulfil this condition. Therefore, Doppler laser cooling is applied for the efficient reduction of the longitudinal velocity spread of the ion beam. Providing sufficient confinement, the transverse ion motion is coupled to the longitudinal motion and cooling of all degrees of freedom is achieved.

[1] Present address: NIST, Boulder, CO, USA.

The PALLAS storage ring has been used for the emulation of synchrotrons [8] mapping the focusing parameters required to attain and maintain coasting [6, 7] and bunched [9, 10] crystalline ion beams. For bunched ion beams the ion current is additionally modulated by a harmonic pseudo-potential in the co-moving system, the so-called 'bucket' potential, thereby splitting and compressing the beam into 'bunches'. Except for the collective motion of the ions in the beam, this situation is equivalent to the situation commonly found in linear Paul traps (see, e.g., [11]). Yet, the length of the bunches can be considerably larger as compared to the typical situation of a stationary ion crystal in a linear Paul trap, challenging theoretical models as will be shown. We first recapitulate the experimental methods to create bunched crystalline ion beams, which have been described in more detail elsewhere [9, 10], and then discuss novel results on the shape and the structure of these crystalline ion bunches as a function of the strength of the longitudinal and the transverse confinement.

2. Experimental setup

The PALLAS storage ring resembles a quadrupole ion guide, bent into a circle of $C = 2\pi \times R = 2\pi \times 57.5\,\mathrm{mm}$ circumference [12, 13]. Typically, a radio frequency $\Omega = 2\pi \times 6.3\,\mathrm{MHz}$ with an amplitude of $U_{rf} = 300\,\mathrm{V}$ is applied between the ring-shaped quadrupole electrodes with an aperture radius of $r_0 = 2.5\,\mathrm{mm}$. Stored $^{24}Mg^+$ ions of mass m and charge e then experience a time-averaged harmonic pseudo-potential $\Psi(r) = \Psi_0 r^2 / r_0^2$ with a depth of $\Psi_0 = qU_{rf}/8$, where $q = 2eU_{rf}/\left(m\Omega^2 r_0^2\right)$ denotes the stability parameter of the Mathieu differential equation [14] and has a typical value of $q = 0.25$. This potential transversely confines the ions along the orbit and leads to a secular frequency $\omega_{\mathrm{sec}} = q\,\Omega/\sqrt{8}$.

Furthermore, the longitudinal ion motion can be manipulated by the use of 16 individual drift tubes. With an effective length of $L = 22\,\mathrm{mm}$ each, they enclose the whole ion orbit.

Two laser beams, addressing the Doppler-shifted $3s\,^2S_{1/2}$–$3p\,^2P_{3/2}$ transition of the $^{24}Mg^+$ ions, are used for the acceleration of the ions, one co-propagating with the ion beam, one counter-propagating. During acceleration the frequency ω_1 of the first laser is continuously increased at a tuning rate of 5 GHz s^{-1}. The frequency ω_2 of the second laser is kept fixed, determining the final velocity of the coasting beam of typically $v \approx 2600\,\mathrm{m\,s^{-1}}$. The longitudinal velocity spread of the ion beam is efficiently reduced by the friction force that results from the combination of both accelerating and decelerating laser forces [1, 5–7].

The fluorescence light of laser-cooled ions is detected with a fast photo-multiplier. Furthermore, time-averaged images of the beam can be recorded with an intensified CCD video camera. While these images represent a direct measurement of the transverse beam profile, the longitudinal profile of an ion bunch is measured by recording the photo-multiplier signal in phase with the bunching voltage [10] applied to one of the drift tubes (as described below). The spatial ion distribution in the bucket is then derived from the recorded temporal distribution of fluorescence photons.

3. Bunching of ion beams in PALLAS

A sinusoidal potential at a bunching frequency of $\omega_b \approx 2\pi \times 40\,\mathrm{kHz}$ (harmonic number $h = 6$) and amplitude U_0 of a few mV is applied to one of the drift tubes of length L for the control of the spatial longitudinal ion distribution [9, 10]. If the bunching frequency is tuned to a harmonic number h of the revolution frequency $\omega_{\mathrm{rev}} = 2\pi \times v/C$, an ion propagating with the synchronous velocity $v_s = C\omega_b/(2\pi h)$ experiences no longitudinal force while ions

with higher velocities will be decelerated and vice versa [8]. Individual ions oscillate in h co-moving longitudinal pseudo-potential wells with an effective potential depth [9, 10] of

$$U_b = 2U_0 \sin(\pi h L/C) \tag{1}$$

with the synchrotron frequency

$$\omega_{\mathrm{syn}} = 2\pi \times \sqrt{\frac{eU_b h}{2\pi C^2 m}}. \tag{2}$$

For the case of bunched beams, the friction force providing the longitudinal cooling can be generated with a combination of the decelerating force of the counter-propagating laser beam and the restoring pseudo-force of the bucket [15, 16], again similar to the situation of laser cooling of stationary ions in the harmonic well of a linear trap. In this regime of a bunched beam cooled with only the decelerating laser beam at fixed frequency ω_2, the bunching frequency has to be carefully adjusted, so that the synchronous velocity v_s comes to lie slightly below the velocity corresponding to the Doppler-shifted laser resonance (see also [9, 10]). The synchrotron motion is efficiently damped and the ions are cooled to the synchronous velocity, but shifted out of the bucket centre by the laser force. Crossing this resonance condition immediately leads to an inverse situation where the synchrotron motion of the ions is increased as then ions are driven out of the bucket by the decelerating laser force.

Thus, the experimental procedure used for the attainment of crystalline bunched beams is the following: to prevent any ion losses due to initial mis-adjustments of the frequencies, ions are (re-)accelerated by the continuously scanning co-propagating laser beam as for the previous case of the acceleration of the coasting beam until the fine adjustment of the bunching frequency ensures efficient cooling by the counter-propagating laser beam inside the comparatively shallow bucket. Once this point is reached, no ions are lost from the bucket anymore and the accelerating laser beam can be shut off.

4. Shape and structure of ion crystals in the bucket

Large stationary ion crystals confined in linear Paul traps by harmonic potentials of different strengths in the transverse and longitudinal directions form spheroids of constant charge density which can be characterized [11, 17, 18] by their aspect ratio

$$\alpha = \frac{L_b}{D_b}. \tag{3}$$

The full longitudinal length L_b and the full transverse width D_b refer to the distances of the outermost ions in the longitudinal and transverse directions. For a comparison with experimental data of crystalline beams, where single ions are presently not resolved, D_b and L_b have to be replaced by statistical quantities, leading to $\alpha^* = L_{\mathrm{FWHM}}/(4\sigma)$. As described in [6], the full transverse width of the beam is approximated by four times the width σ^c of a Gaussian, from which an overall resolution of the imaging system (here $\sigma^0 = 4.8\,\mu$m) is subtracted according to $\sigma = \sqrt{(\sigma^c)^2 - (\sigma^0)^2}$. The FWHM bunch length [10] L_{FWHM} is used for the description of the length of the bunch.

A more intriguing image of the spatial distribution of the bunch (similar to the images of stationary ion crystals) could clearly be acquired by strobing the intensified camera synchronously with the bunching voltage. Yet, the accumulation of consecutive images after each revolution of the bunch is very time consuming and therefore requires long-term stability of the cooling lasers that cannot be guaranteed with the present setup. For an exposure time of 10 ns per image, the integration time would be of the order of 25 min and thus this

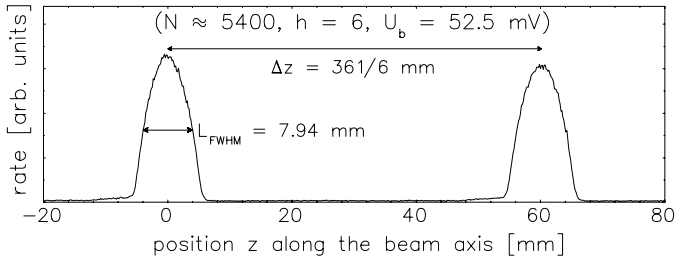

Figure 1. Longitudinal beam profile ($\beta = 282 \times 10^3, \alpha^* = 826$) showing two consecutive ion bunches. The parabolic shape of the bunches indicates a space-charge-dominated beam. The distance of the two bunches is given by $\Delta z = C/h$. The length of the bunches corresponds to a compression of $\Delta z/L_{\mathrm{FWHM}} = 7.6$, while the transverse beam radius is $2\sigma = 9.6\,\mu$m.

technique would not allow the kind of systematic investigations presented here. Nevertheless, the required improvements of the experimental setup are planned to be made in the near future.

In the PALLAS storage ring extremely elongated crystal structures confined in the bucket potential well with a length of the order of 10 mm and a width of only several μm are investigated. In this regime the shape of the crystal is no longer adequately described by a spheroid as in the cold fluid model, where an analytical expression for the dependence of α on the trap parameter β, the ratio of the transverse to the longitudinal confinement strength, has been derived [17–19].

Still, the aspect ratio α should depend on β for the case of bunched beams where the confinement strength is characterized by

$$\beta = \frac{\omega_\perp^2}{\omega_z^2} = \frac{\omega_{\mathrm{sec}}^2}{\omega_{\mathrm{syn}}^2}. \tag{4}$$

The structure of an ion crystal consisting of $N_b = N/h$ particles is uniquely determined [12, 20] by the dimensionless linear density

$$\lambda(z) = n(z)a_{ws} \qquad a_{ws} = \left[\frac{1}{4\pi\epsilon_0}\frac{3e^2}{2m\omega_{\mathrm{sec}}^2}\right]^{1/3} \tag{5}$$

where $n(z) = \Delta N/\Delta z$ denotes the local linear ion density and a_{ws} the Wigner–Seitz radius, which is a measure of the average inter-ion spacing as a function of the strength of the transverse confinement. For infinitely long ion crystals, only 'truly' realized for the case of coasting beams, a transition from a one-dimensional string of ions into a two-dimensional zig-zag pattern is expected for $\lambda(z) = \lambda = 0.71$ [20].

5. Longitudinal spatial beam profiles

A typical longitudinal profile of a bunched crystalline beam in the PALLAS storage ring is shown in figure 1. The inverse parabolic form of the two consecutive ion bunches indicates that the inter-ion Coulomb repulsion is in equilibrium with the confining forces of the harmonic longitudinal pseudo-potential and that the shape of the bunch is no longer determined by its temperature.

Two different models are compared to the experimental results in the following discussion. In both models, the linear ion density $n(z)$ is well described by an inverse parabola [21], for

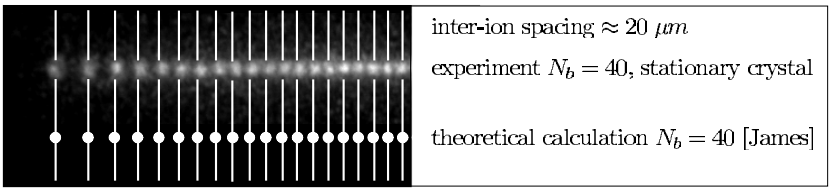

Figure 2. Fluorescence image of the left half of a stationary ion crystal in the storage ring PALLAS with $N_b = 40$ ions compared to the corresponding theoretical calculation following James [23]. The string was confined in harmonic potentials in both the transverse and longitudinal directions. The trap parameter was $\beta \approx 1340$ ($\omega_z = 2\pi \times 15$ kHz, $\omega_{\rm sec} = 2\pi \times 550$ kHz). Note that the weak longitudinal confinement was generated with the drift tubes also used for the bunching of beams.

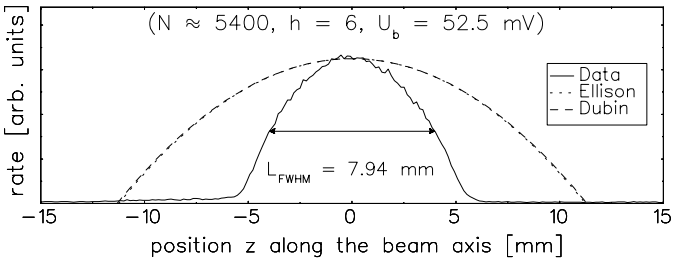

Figure 3. Enlarged longitudinal profile of the bunched crystalline ion beam presented in figure 1. The measured profile is compared to a parabolic profile where the length corresponding to a one-dimensional ion string [21] (almost identical to the one corresponding to a non-crystalline space-charge-dominated beam [22]) is used.

which one can substitute $L_{\rm FWHM}$ by $L_b/\sqrt{2}$. For space-charge dominated but non-crystalline bunched beams, Ellison *et al* [22] derived a total bunch length of

$$L_{\rm Ellison} = \left[\ln\left(\frac{r_0}{2\sigma}\right) 12 N_b \frac{e}{\epsilon_0}\frac{R^2}{U_b h}\right]^{\frac{1}{3}}. \tag{6}$$

Note that the dependence of the length on the ratio of the aperture radius r_0 to the transverse beam radius 2σ indicates that this model describes three-dimensional ion bunches in a conducting beam pipe.

On the other hand, the model of Dubin [21] describes a one-dimensional ion string trapped in a longitudinal harmonic potential. The corresponding total bunch length amounts to

$$L_{\rm Dubin} = \left[\left(\ln(6N_b) + \gamma - \frac{7}{2}\right) 12 N_b \frac{e}{\epsilon_0}\frac{R^2}{U_b h}\right]^{\frac{1}{3}} \tag{7}$$

where $\gamma \approx 0.5772$ is Euler's constant and parameters are adopted for the conditions at the PALLAS storage ring. Starting from the cold fluid model [17, 18], this approach takes into account the long-range order of the ion string which is especially relevant for small numbers of ions ($N_b \lesssim 200$) in the bunch, but gives results for the bunch length similar to those of equation (6) for N_b of the order of 1000. Equation (7) was shown to be in good agreement with direct calculations of the ion positions [21, 23]. For illustration purposes, figure 2 shows an image of the left half of a stationary ion string ($N_b = 40$) stored in PALLAS. The ion positions are compared to a direct calculation following James *et al* [23], nicely describing the measurement.

In surprising contrast, figure 3 shows a comparison of the longitudinal profile of a bunched crystalline ion beam ($N_b \approx 1000$) with the two models. Compared to equations (6) and (7),

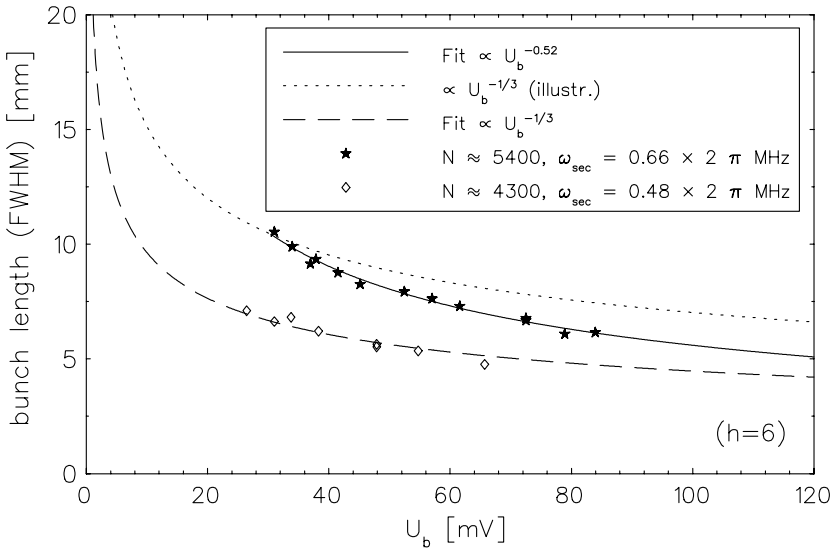

Figure 4. Deviation from the dependence $L_{\mathrm{FWHM}} \propto U_b^{-1/3}$ of the FWHM bunch length L_{FWHM} at a given bunching voltage U_b for a bunched crystalline ion beam (filled stars). The dotted curve follows the expected $U_b^{-1/3}$ scaling to illustrate the difference from the experimental result, yet, the absolute length is fitted to the first data point. For reasons of comparison the bunch lengths (2σ of a Gaussian profile) of a hot, non-space-charge-dominated beam (open rhombs) have been added to the plot.

the length of the bunch is about a factor of 2 smaller than expected, considerably increasing the phase-space density of the ion beam.

At this point, the most obvious difference between the crystalline bunches presented here and the stationary crystal shown in figure 2 lies in the number of ions involved and in the corresponding overall length.

Bunch lengths measured at different bunching voltages are presented in figure 4. The bunch length for a crystalline ion string should depend on the depth of the longitudinal confining potential as $L_b \propto U_b^{-1/3}$ [21], provided no changes in the structure of the crystal, which might change its compressibility ($\propto \mathrm{d}L_b/\mathrm{d}U_b$), take place during the compression. Reflecting the harmonic confinement, the same dependence should hold true for non-crystalline space-charge-dominated beams [22] and for emittance-dominated hot beams. Figure 4 depicts the deviation from this dependence found in the experiment. At present, this behaviour can only be attributed to local changes in the crystal structure. In a zig-zag configuration another degree of freedom transverse to the direction of the beam propagation opens and the ions are pushed aside by the Coulomb repulsion when the longitudinal confinement is increased. For sufficiently long crystals, the central part of the crystal can undergo such a transition to a zig-zag with a rather constant linear density of $0.8 \lesssim \lambda \lesssim 0.9$, while the rest of the crystal remains in the string configuration where λ gradually varies with z.

As an illustration, figure 5 shows an image of a stationary ion crystal recorded in the PALLAS storage ring which exhibits the onset of such a structural transition. The transition is accompanied by a considerable decrease in the crystal length. An increase in the longitudinal confinement causes more ions to flip into a zig-zag configuration and the ion crystal becomes shorter more quickly than expected according to $L_b \propto U_b^{-1/3}$. Yet, the absolute value of the length and thus the discrepancy with the much larger theoretical value cannot be attributed to this effect.

Figure 5. Fluorescence image of the left half of a stationary ion crystal with $N_b \approx 68$ ions in the PALLAS storage ring. The gradual transition from a string-like structure on the outside to a zig-zag inside the crystal is visible. The inter-ion spacing is comparable to that in figure 2, the trap parameter is $\beta = 73$ ($\omega_{\mathrm{sec}} = 2\pi \times 180\,\mathrm{kHz}$, $\omega_z = 2\pi \times 21\,\mathrm{kHz}$).

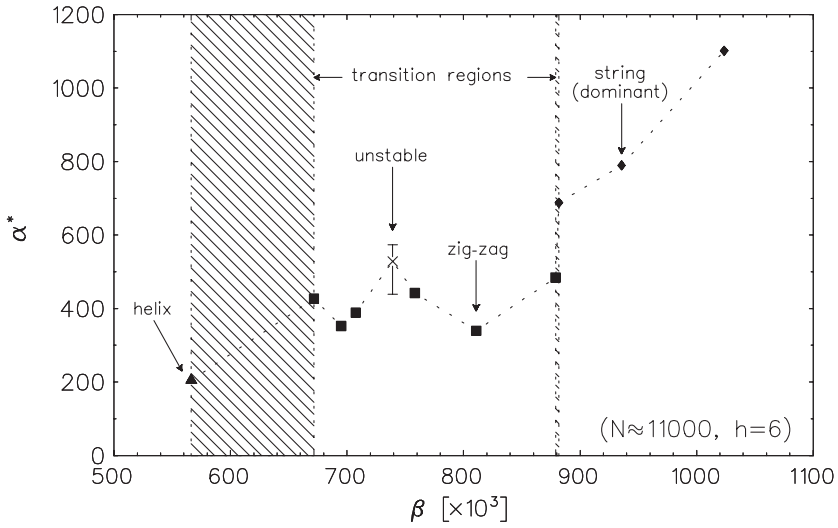

Figure 6. Mapping of the structural transition of a bunched crystalline ion beam.

6. Mapping the transition from string to zig-zag

Experiments have shown that the threshold value of $\lambda = 0.71$, established for the transition from a string to a zig-zag [20] in infinite systems, also roughly holds for a local transition in longitudinally confined ion crystals [5, 12]. To investigate this transition in bunched crystalline beams, careful changes were applied to the rf potential depth U_{rf} and the bunching voltage U_b to approach the critical trap parameter corresponding to the transition. Thus, each data point in figure 6 corresponds to a different combination of these voltages chosen independently for each point to maintain a stable beam. The dotted line connecting the different data points in figure 6 is solely meant to guide the eye.

Although for a parabolic profile of the linear density $n(z)$, obviously, parts of the ion crystal can evolve into a zig-zag structure below an average linear density of $\bar{\lambda} = (1/L_b)\int_{-L_b/2}^{+L_b/2} a_{ws} n(z)\,\mathrm{d}z = 0.71$, a sharp transition was observed at a distinct value of $\beta \approx 880 \times 10^3$ as depicted in figure 6. The average linear density amounts to $\bar{\lambda} \approx 0.83$ at this transition point. This structural transition is identified by a sudden broadening of the width of the beam similar to the case of coasting beams [6]. The transverse beam size changes significantly when a 'full' structural transition from a string to a zig-zag configuration takes place. For the case of ion bunches, only a minor part is assumed to remain in the string configuration in contrast to the situation illustrated in figure 5. Previous systematic studies of the transverse beam size of different crystal structures for coasting beams [6, 7] allow the

three structural regimes to be distinguished, string, zig-zag and helix, although the transverse beam size has to be reconstructed from a time-averaged picture, where longitudinal changes in the crystal structure are smeared out.

Predictions from MD simulations ($N_b < 500$) [19] and from the cold fluid model [24] for the trap parameter value at which the transition from a string to a zig-zag should occur exist, namely

$$\beta^{(1)}_{\text{Schiffer}}(N_b) = 0.395 N_b^{1.73} \qquad N_b < 500 \quad [19] \tag{8}$$

and

$$\beta^{(1)}_{\text{Dubin}}(N_b) = \frac{(3x_1 N_b)^2}{64(\ln(6N_b) + \gamma - 13/5)} \qquad x_1 \approx 2.05 \quad [24]. \tag{9}$$

The predicted values, $\beta_{\text{Schiffer}}(N_b) = 175 \times 10^3$ and $\beta_{\text{Dubin}}(N_b) = 273 \times 10^3$ for $N_b = 11\,000/6$ both differ considerably from the experimental result, which is consistent with previously published PALLAS data [10].

Further changes in the transverse width were observed for different zig-zag configurations, leading to the different values of α^* in figure 6. For certain values of the trap parameter the beam was found to be unstable, indicated by the cross in figure 6, possibly due to recurring structural changes from a string to a zig-zag. The size of the error bars refers to the maximum and minimum values measured and is of the same order of magnitude as the differences in α^* for the zig-zag structures.

7. Conclusion and outlook

First systematic studies of the length and width of bunched crystalline ion beams were performed in the PALLAS rf quadrupole storage ring. The dependence of the bunch length on the bunching voltage has been found to strongly and surprisingly differ from theoretical predictions for pure crystalline strings. The different scaling with increasing longitudinal confinement can be qualitatively explained by the gradual formation of a crystal structure dominated by an ion string, but including a small zig-zag contribution. For these string-like crystalline bunched beams the absolute bunch length has always been found to be at least a factor of 2 shorter than that expected from the literature for non-crystalline space-charge-dominated beams or large one-dimensional ion strings, notably a very favourable effect. Such a shorter bunch length might even hint at a release of energy related to the phase transition [25]. Yet, the quantitative dependence of the bunch length on the particle number remains to be investigated.

Moreover, a sharp transition at $\bar{\lambda} = 0.83$ from a string-like structure of the ion crystal to a zig-zag has been observed, similar to our previous observations [9, 10], and mapped as a function of the trap parameter. This trap parameter value of $\beta \approx 880 \times 10^3$ has been found to be considerably different from theoretical predictions. Since the predictions for the length of a pure ion string and the value of the trap parameter at the transition from a string to a zig-zag structure are closely related [24], a final explanation of the obvious discrepances between the experimental results presented here and the theoretical predictions should include aspects of the shape and structure of highly elongated crystals as well as of the dynamics of the structural transition.

For the ongoing investigation of mixed crystalline structures in bunched beams, the systematic mapping of a wider range starting from an unambiguous string to a final zig-zag structure is foreseen. It is planned to further investigate the $L_b \propto U_b^{-1/3}$ scaling and its dependence on the ion number N_b for bunched crystalline ion strings. Additionally, MD

calculations are currently prepared to investigate the string to zig-zag transition in a bunched ion beam of $N_b \gtrsim 1000$.

Acknowledgments

This work has been supported by the DFG (HA1101/8) and the MLL. We acknowledge fruitful discussions with P Kienle and J P Schiffer and generous technical support by R Neugart.

References

[1] Schramm U *et al* 2002 *Plasma Phys. Control. Fusion* **44** B375
[2] Schiffer J P and Kienle P 1985 *Z. Phys.* A **321** 181
Rahman A and Schiffer J P 1986 *Phys. Rev. Lett.* **57** 1133
[3] Habs D and Grimm R 1995 *Ann. Rev. Nucl. Part. Sci.* **45** 391
[4] Maletic D M and Ruggiero A G (ed) 1996 *Crystalline Beams and Related Issues* (Singapore: World Scientific)
[5] Schätz T *et al* 2001 *Nature* **412** 717
[6] Schramm U *et al* 2002 *Phys. Rev.* E **66** 036501
[7] Schramm U *et al* 2003 *Proc. Trapped Charged Particles and Fundamental Interactions* (*J. Phys. B: At. Mol. Opt. Phys.* **36** at press)
[8] Bryant P J and Johnson K 1993 *Circular Accelerators and Storage Rings* (Cambridge: Cambridge University Press)
[9] Schramm U *et al* 2001 *Phys. Rev. Lett.* **87** 184801
[10] Schramm U *et al Proc. 5th Int. Conf. on Nuclear Physics at Storage Rings (Phys. Scr.* at press*)*
[11] Hornekær L and Drewsen M 2002 *Phys. Rev.* A **66** 013412
[12] Birkl G *et al* 1992 *Nature* **357** 310
[13] Schätz T *et al* 2003 *Appl. Phys.* B at press
[14] Gosh P G 1995 *Ion Traps* (Oxford: Clarendon)
[15] Hangst J *et al* 1995 *Phys. Rev. Lett.* **74** 4432
[16] Miesner H-J *et al* 1996 *Nucl. Instrum. Methods* A **383** 634
Eisenbarth U *et al* 2000 *Nucl. Instrum. Methods* A **441** 209
[17] Turner L 1987 *Phys. Fluids* **30** 3196
[18] Dubin D H E 1993 *Phys. Fluids* B **5** 295
[19] Schiffer J P 1993 *Phys. Rev. Lett.* **70** 818
[20] Hasse R W and Schiffer J P 1990 *Ann. Phys., NY* **203** 419
[21] Dubin D H E 1997 *Phys. Rev.* E **55** 4017
[22] Ellison T J P *et al* 1993 *Phys. Rev. Lett.* **70** 790
[23] James D F V 1998 *Appl. Phys.* B **66** 181
[24] Dubin D H E 1993 *Phys. Rev. Lett.* **71** 2753
[25] Schiffer J P 2002 *Phys. Rev. Lett.* **88** 205003